

Supporting information

In-situ polymerization of 1,3-dioxolane and formation of fluorine/boron-rich interfaces enabled by film-forming additives for long-life lithium metal batteries

Ting Li^a, Kai Chen^a, Borui Yang^a, Kun Li^a, Bin Li^a, Miao He^b, Liu Yang^a, Anjun Hu^{a,b}, Jianping Long^{a*}*

^a College of Materials and Chemistry & Chemical Engineering, Chengdu University of Technology, 1#, Dongsanlu, Erxianqiao, Chengdu 610059, Sichuan, P. R. China

^b State Key Laboratory of Electronic Thin Films and Integrated Devices, University of Electronic Science and Technology of China, Chengdu, 610054, Sichuan, P. R. China

* Corresponding author: anjunhu@cdut.edu.cn (Anjun Hu); longjianping@cdut.cn (Jianping Long)

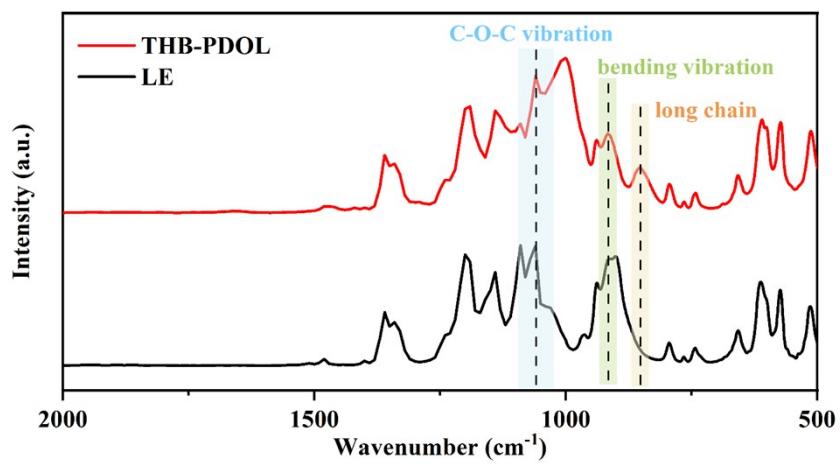


Figure S1. FTIR spectra of LE solvent, THB-PDOL

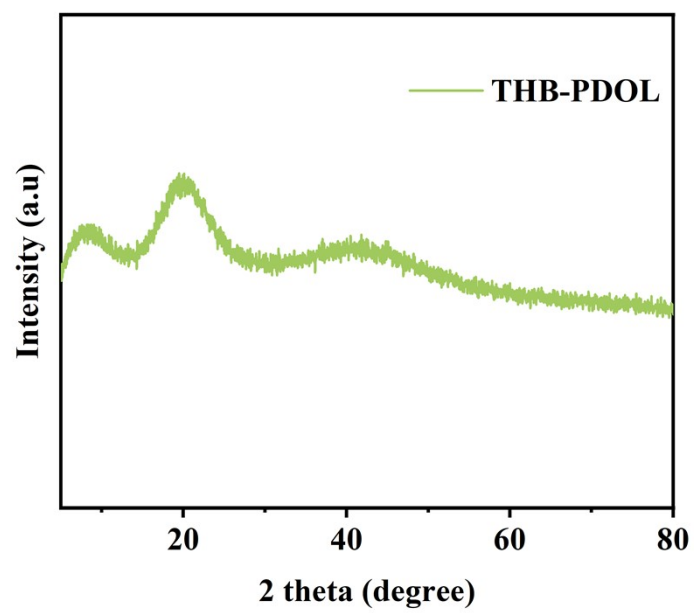


Figure S2. XRD pattern of THB-PDOL.

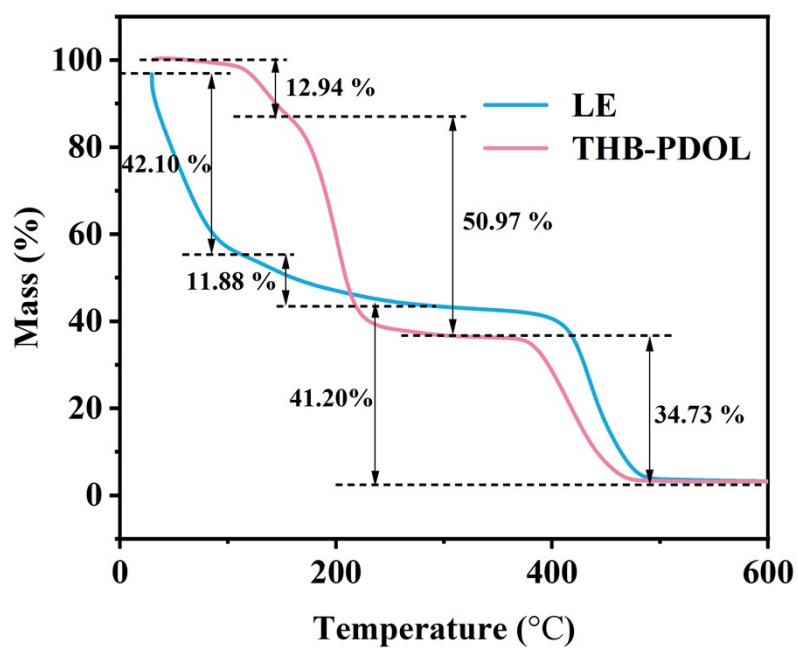


Figure S3. TG profiles of LE and THB-PDOL.

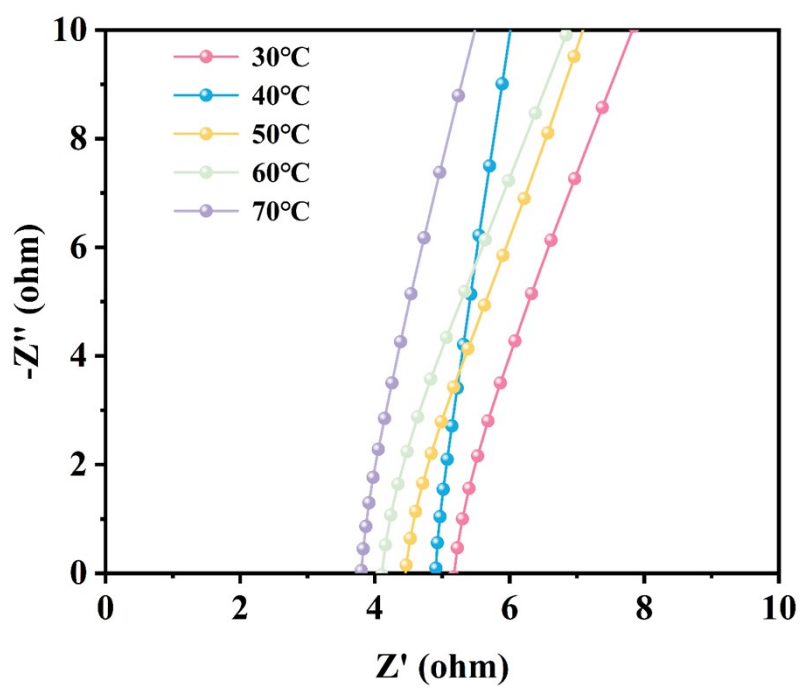


Figure S4. Impedance diagrams of THB-PDOL at different temperatures.

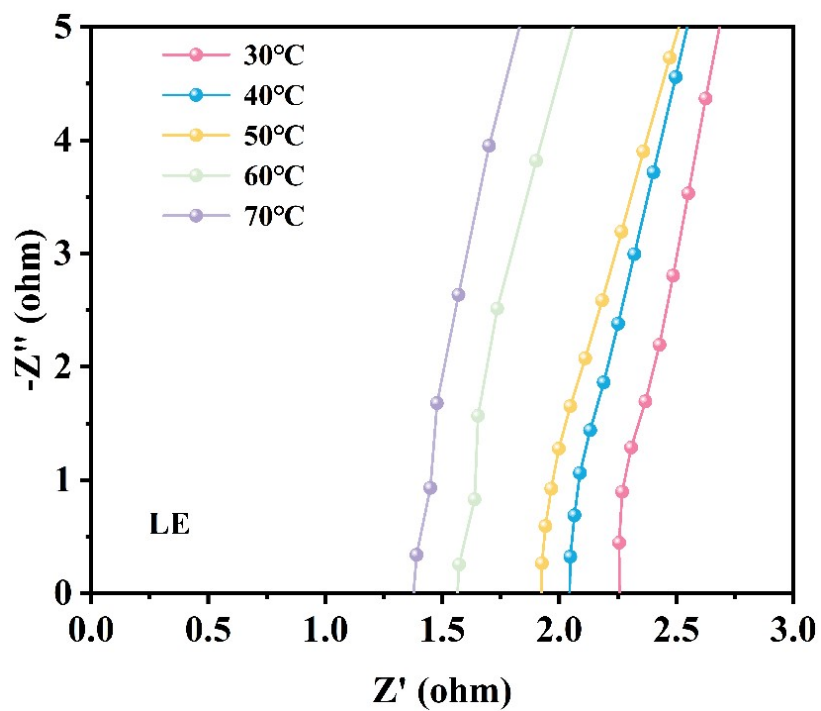


Figure S5. Impedance diagrams of LE at different temperatures.

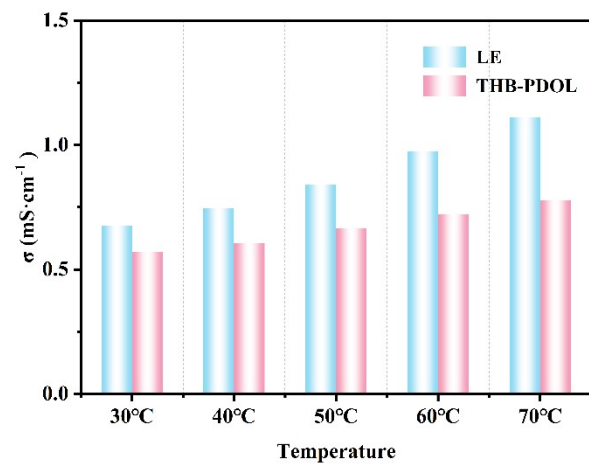


Figure S6. Ionic conductivity of LE and THB-PDOL at different temperatures.

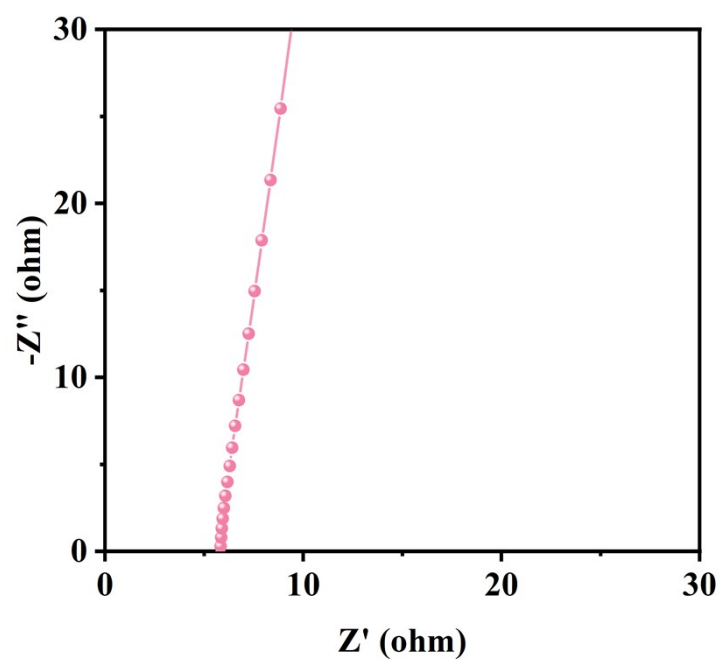


Figure S7. Impedance diagrams of THB-PDOL at 25°C. The calculated ionic conductivity of THB-PDOL is $5.074 \times 10^{-4} \text{ S cm}^{-1}$.

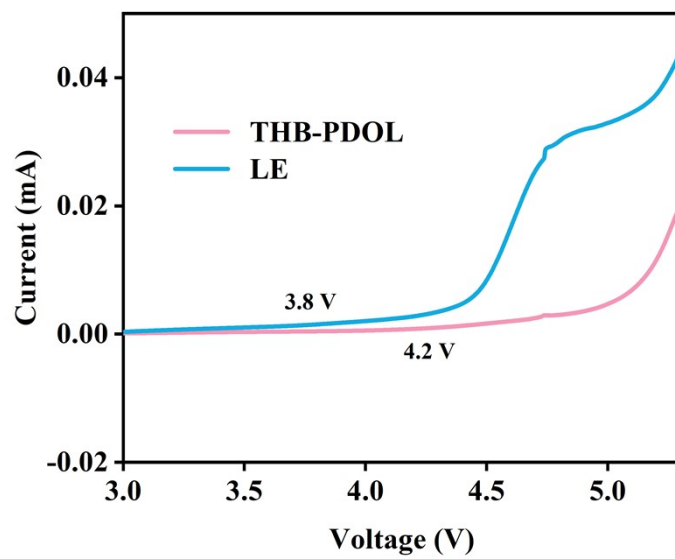


Figure S8. Linear sweep voltammetry (LSV) curves of THB-PDOL, and LE at room temperature.

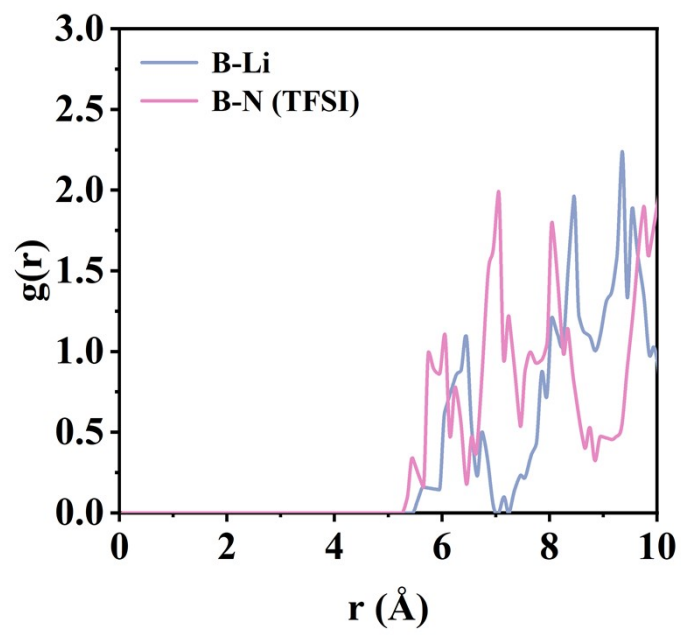


Figure S9. Calculation of the radial distribution function $g(r)$ for lithium salt anions and cations in THB-PDOL.

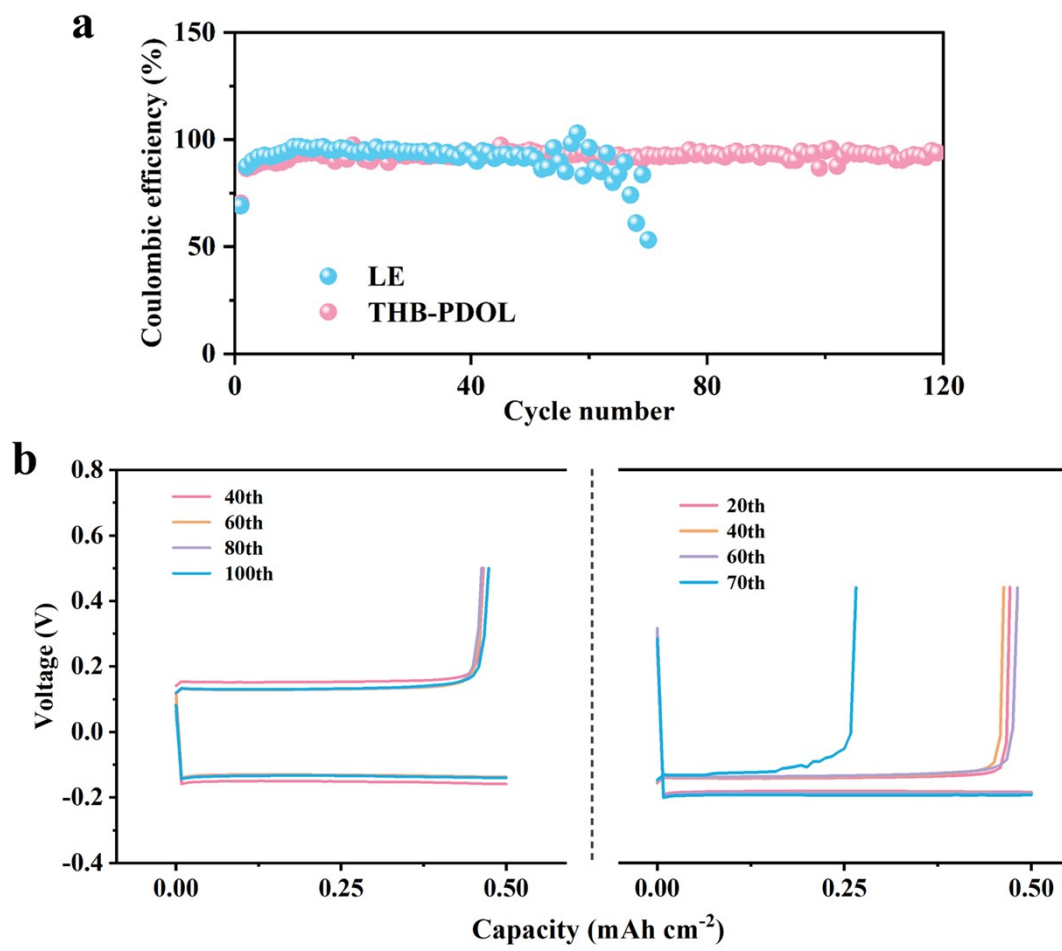


Figure S10. (a) Coulombic efficiency of Li||Cu asymmetric cells for THB-PDOL and LE. (b) and corresponding voltage profiles with THB-PDOL and LE.

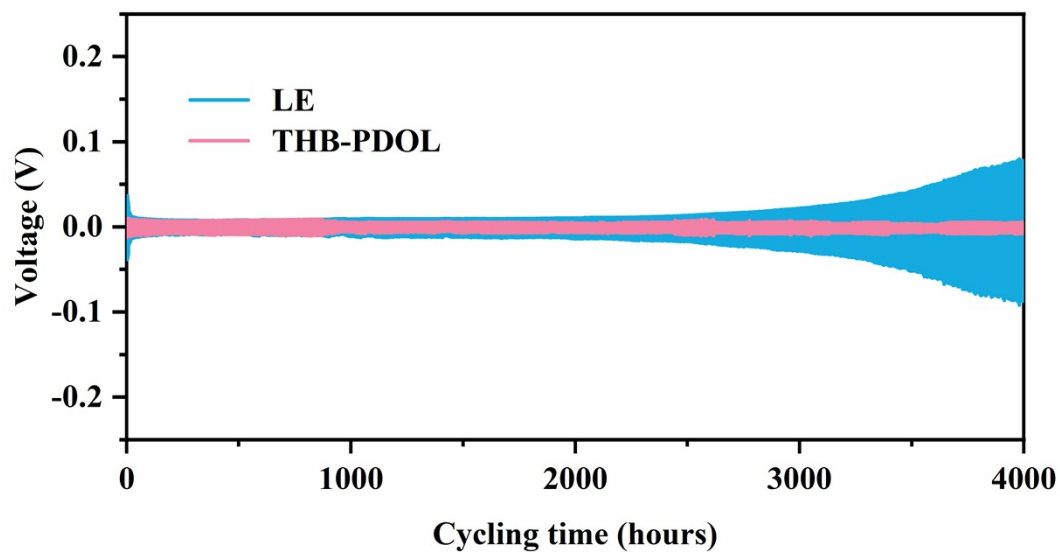


Figure S11. Voltage profiles of Li||Li symmetric cells of THB-PDOL and LE at a current of 0.1 mA cm^{-2} at room temperature.

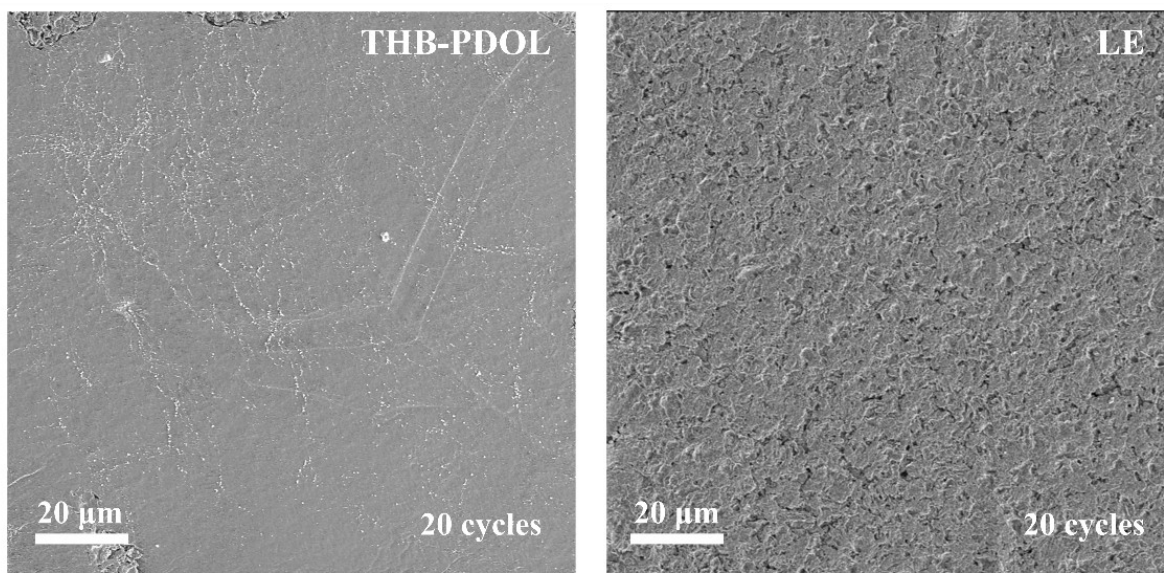


Figure S12. SEM images of lithium metal anode surfaces of THB-PDOL and LE after 20 cycles at current density of 0.5 mA cm^{-2} with a capacity of 0.5 mAh cm^{-2} .

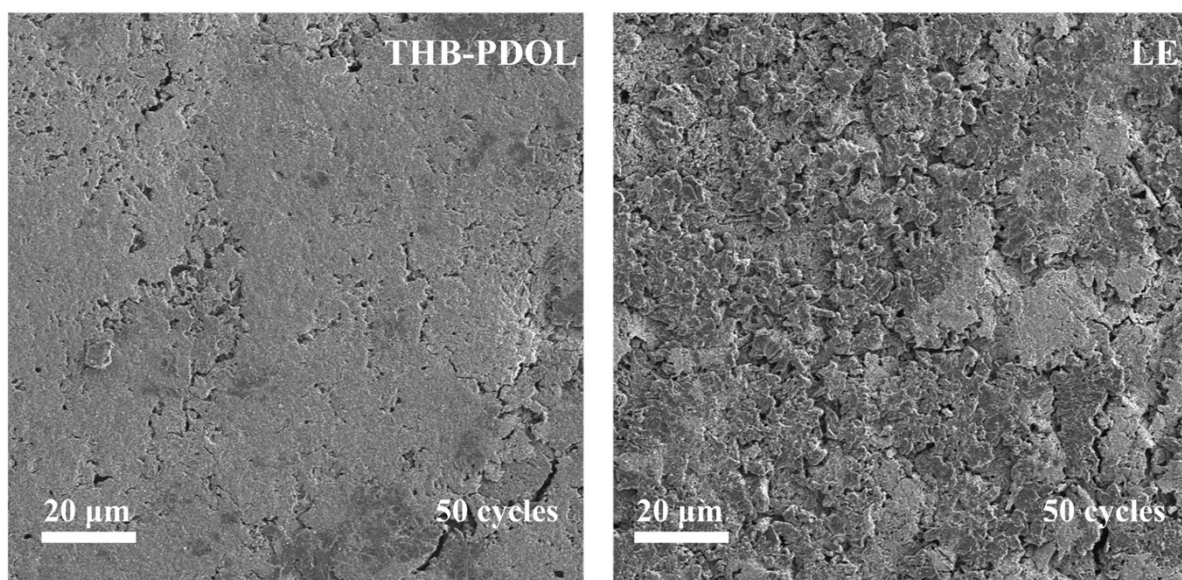


Figure S13. SEM images of lithium metal anode surfaces of THB-PDOL and LE after 50 cycles at 0.5 mA cm^{-2} , 0.5 mAh cm^{-2} current densities, Scale bar: $20 \text{ }\mu\text{m}$.

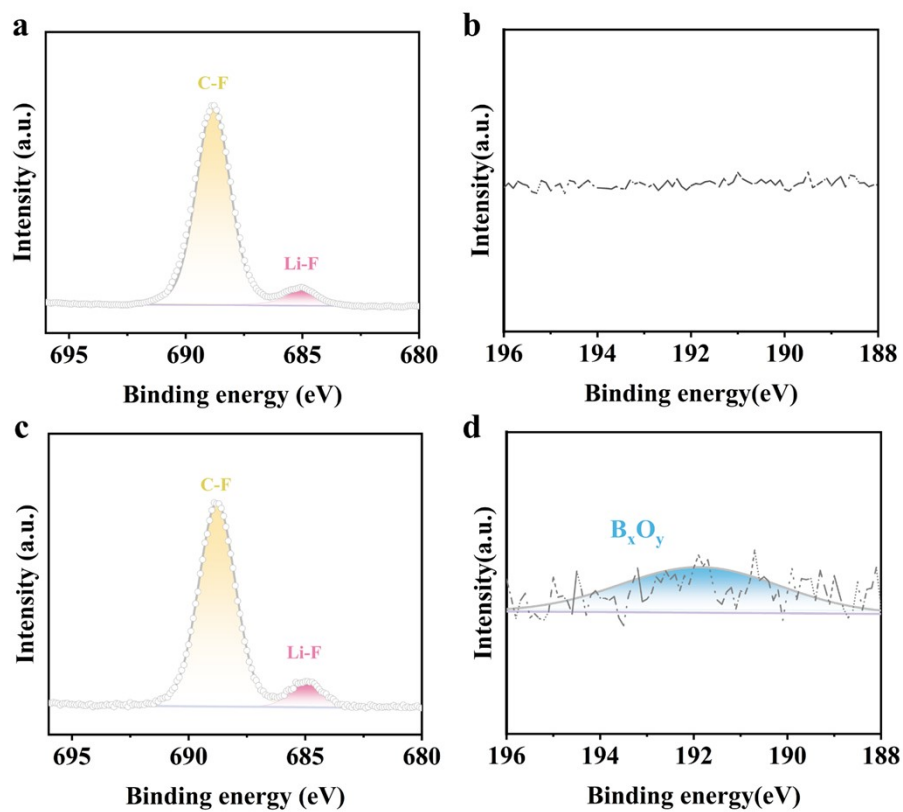


Figure S14. XPS spectra corresponding to F 1s, B 1s of Li metal after 20 cycles of Li||Li symmetrical cells at 0.5 mA cm⁻² with a capacity of 0.5 mAh cm⁻² in (a and b) LE and (c and d) THB-PDOL.

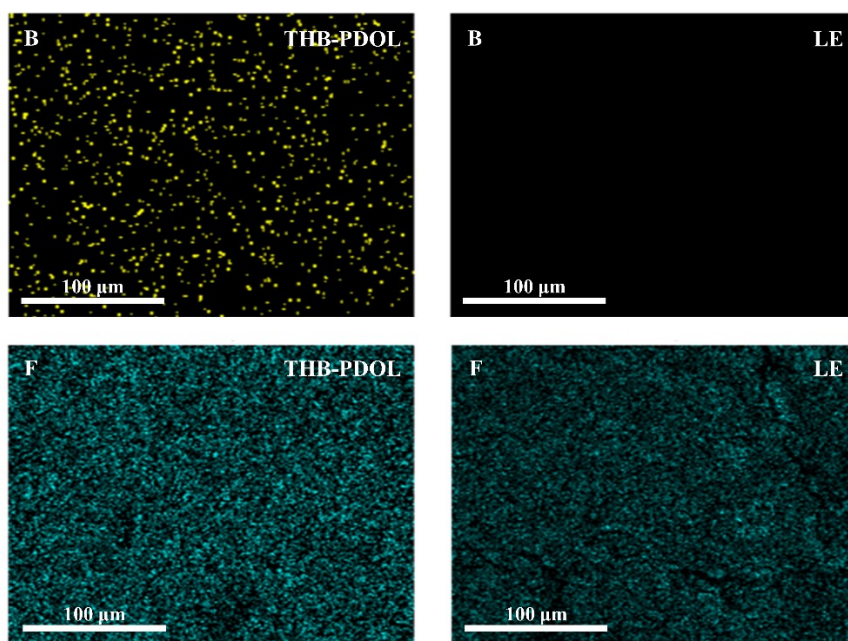


Figure S15. EDS mapping of lithium anode surface after cycling

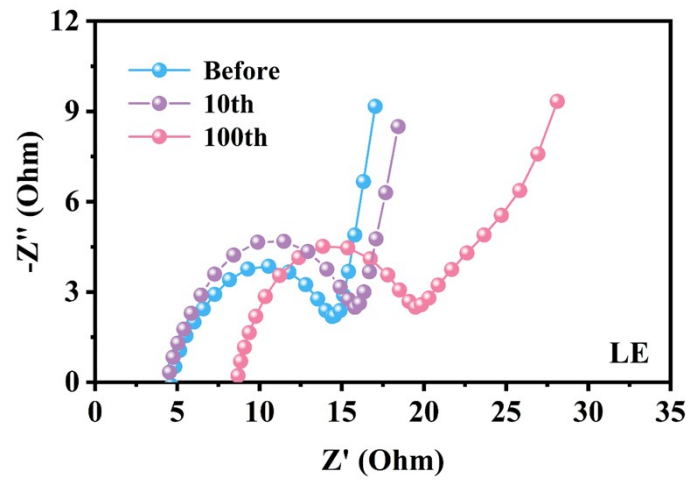


Figure S16. EIS curve of Li||LE||LFP at 1 C.

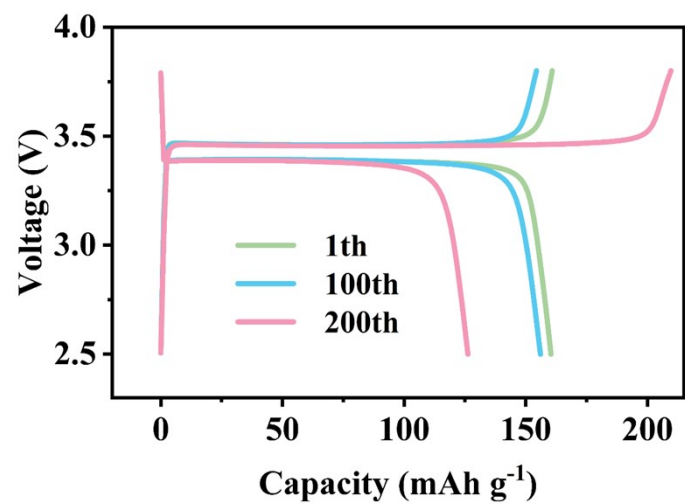


Figure S17. The charge–discharge voltage curve of Li||LE||LFP full cell during 200 cycles.

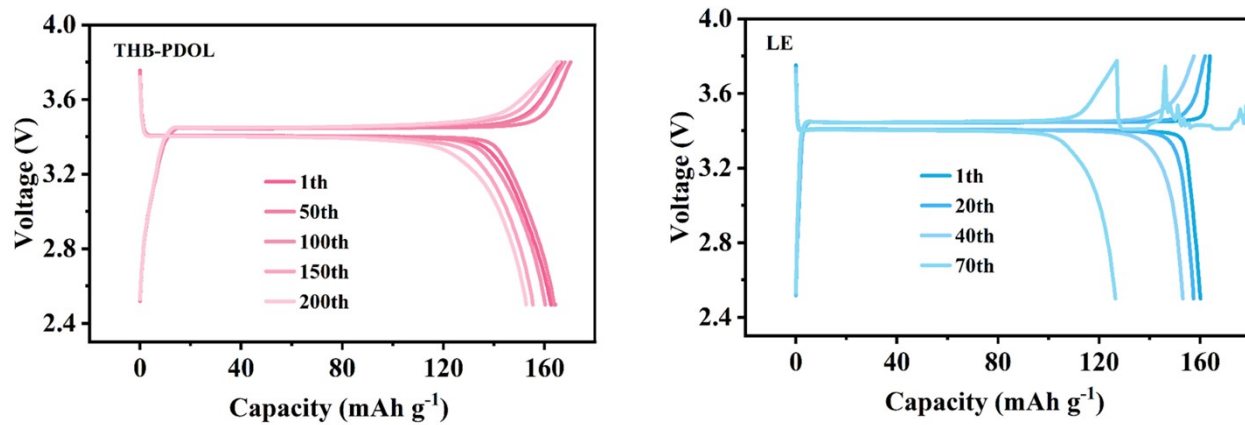


Figure S18. The charge–discharge voltage curve of Li||THB-PDOL||LFP and Li||LE||LFP full cells at 60°C.

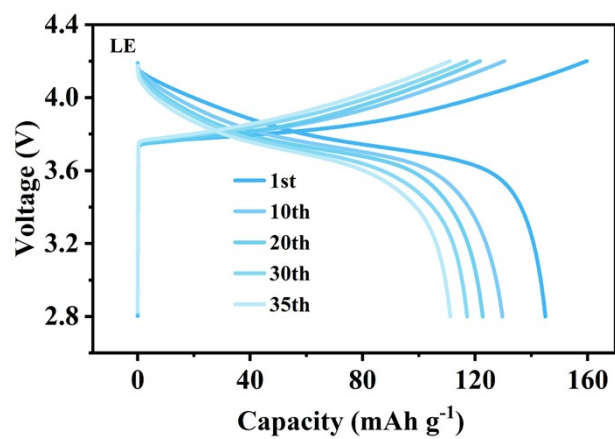
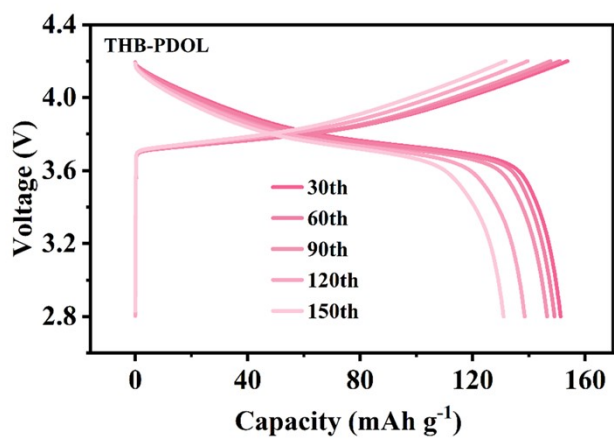


Figure S19. The charge–discharge voltage curve of Li||THB-PDOL|NCM523 and Li||LE|NCM523 full cells.

Table S1. Atomic concentration of B elements.

Sample	At% (B)	At% (F)
LE	0.00	18.68
THB-PDOL	4.06	23.08